Does contrast ultrasound dispersion imaging reveal changes in tortuosity? : a comparison with acoustic angiography

Does contrast ultrasound dispersion imaging reveal changes in tortuosity? A comparison with acoustic angiography

Anastasiia Panfilova[1], Sarah Shelton[2], Ruud JG van Sloun[1], Libertario Demi[1],
Hessel Wijkstra[1,3], Paul Dayton[2], Massimo Mischi[1]
[1]Eindhoven University of Technology, Electrical Engineering Dept, Signal Processing Systems Group
[2]Joint Department of Biomedical Engineering,
University of North Carolina at Chapel Hill and North Carolina State University
[3]Academic Medical Center, University of Amsterdam, Urology Dept

***Abstract*—Higher microvascular density with tortuous and irregular vessels are hallmarks of cancer vasculature. These alterations can be captured by contrast ultrasound dispersion imaging (CUDI) and acoustic angiography (AA) at different scales: CUDI aims at obtaining an implicit measure of structural alteration by determining the dispersion kinetics of contrast agents. At a smaller scale, AA images the vascular architecture by detecting the high-frequency components generated with ultrasound contrast agents (UCA). This work shows the performance of these techniques by imaging cancerous and control regions in 3 rat xenograft models. Furthermore, it investigates the diagnostic value of the vascular features extracted using CUDI and AA with the aim to answer the question: does CUDI reveal changes in vascular tortuosity?**

***Index Terms*—Cancer, Acoustic angiography, Contrast-enhanced ultrasound, Ultrasound contrast agents, Dispersion.**

I. Introduction

It has been recognized that cancer tissue can be characterized by a set of alterations [1]. In particular, alterations in the vascular morphology, exhibiting irregular and tortuous vessels, result in heterogeneous flow patterns in the region encompassing the tumor. Moreover, tissue surrounding the tumor is (often) highly vascularized and, therefore, highly perfused, supplying the tumor with nutrients and ensuring its growth. These properties can be registered with dynamic contrast-enhanced ultrasound (DCE-US) techniques, which have been showing promising results in distinguishing malignant from benign tissue [2], [3], [4], [5].

DCE-US captures the intravascular passage of ultrasound contrast agents (UCAs) in a region of interest (ROI). Following the intravenous injection of a UCA bolus, time intensity curves (TICs) are recorded at each pixel in the ROI; they reflect the evolution of the UCA concentration over time, referred to as indicator dilution curve (IDC). Many techniques for UCA quantification are based on the fit of the extracted TICs by analytical models, such as the lognormal, gamma, and local density random walk model (LDRW) [6]. Initially these models were used to extract functional parameters from the fitted curve (mean transit time, area under the time-intensity curve) and assess perfusion. Later, it was recognized that malignant tissue may not always show increased perfusion with respect to benign tissue: the effect of increased microvascular density and arteriovenous shunts may be counterbalanced by irregular diameters and elevated interstitial pressure, creating high resistance to blood flow. Moreover, clinical evidence has shown that cancerous lesions, e.g. in the prostate, can also be iso- or hypo-perfused [4]. This has motivated the development of CUDI [7], [8].

Initially CUDI modeled the UCA bolus passage with a solution of the convective dispersion equation, referred to as modified LDRW model [8]. The dispersion parameter in this solution is influenced by the structure of the pathway where the bolus is observed. Later, spatiotemporal correlation analysis was introduced yielding an indirect measure of dispersion, i.e. the correlation coefficient ρ between TICs at nearby pixels [9]. The performance of this method with respect to cancer detection has already been evaluated in the human prostate [9]. Yet the only validation that has been performed was based on histology-derived microvascular density and cell differentiation. Differently, in this paper we investigated the correlation between CUDI findings and tortuosity measurements as obtained with AA. AA gives an alternative for validation: it images the vasculature directly and enables quantification of tortuosity.

AA allows imaging vessels at a high resolution of 100-200 micrometers at 2 cm with minimal signal from tissue. This technique involves transmission of US waves at frequencies in the order of MHz, close to the UCA bubble resonance frequency. In receive, it records the nonlinear response of the contrast agents in a high frequency range of 25-30 MHz. The advantage of this approach lies in the possibility to quantify vessel morphology using such characteristics as the mean distance metric, the sum of angles metric, and the microvascular density [10]. These measures have been shown to be significantly different for malignant and benign tissue and, therefore, they can be of clinical use in tumor detection and characterization [11]. As a result, AA allows us to evaluate whether vessel tortuosity, as well as microvascular density alterations, can be detected with CUDI.

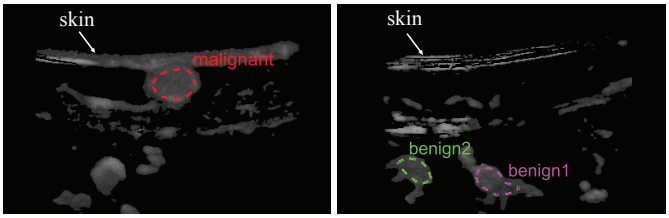

Figure 1: Right- flank with a tumor surrounded by a red contour, left- control flank with 2 benign regions selected for analysis (shown in green and magenta). Regions with power below the threshold of -22 dBs of the maximum intensity are in black.

This work shows the performance of CUDI and AA by imaging fibrosarcoma tumors and control regions in 3 rats. It investigates the diagnostic value of the vascular features extracted using CUDI and AA with the objective of answering the question: does CUDI reveal changes in vascular tortuosity?

II. Methodology

A. Rat Models

Fibrosarcoma tumors were implanted subcutaneously into the flanks of 3 rat specimens (Fischer 344), while their opposite flanks served as controls. After 8 days, DCE-US and AA were performed while the animals were anesthetized with vaporized isoflurane in oxygen. All experiments were approved by the Institutional Animal Care and Use Committee at the University of North Carolina at Chapel Hill.

B. Data acquisition

1) CUDI: A 15L8-S probe was utilized with a Siemens Sequoia in CPS mode, with an insonifying central frequency of 7 MHz. The DCE-US recordings were stored in DICOM format. Contrast wash-in clips were acquired during injection of a bolus of 2×10^8 microbubbles.

2) AA: AA images were acquired with a dual-frequency transducer using an insonifying frequency of 4 MHz, and reception band centered at 30 MHz. Image volumes were acquired using a linear motion stage with 100-μm inter-frame step size. An infusion of 1.5×10^8 microbubbles per minute was administered using a syringe pump (PHD 2000, Harvard Apparatus). As previously described, mapping microvasculature with acoustic angiography yields quantifiable differences between healthy and tumor-bearing tissue volumes in a rodent model [12].

C. Data processing

1) CUDI: Preprocessing of the DCE-US videos included Gaussian filtering with a kernel of 0.13 mm, as performed in [7]. The intensity values of the B-mode images were then converted from logarithmic to linear scale via the known logarithmic compression function. The resulting IDCs were used for computation of the average correlation coefficient for every pixel with respect to its surrounding pixels within a ring-shaped kernel [7]. The obtained correlation coefficient values were depicted with parametric colormaps. Gaussian filtering as well as the spatiotemporal similarity analysis were performed with kernel sizes twice as small as those adopted for humans in the papers mentioned above. This was scaled with the insonifying center frequency.

As the time-scale of the circulation processes is much shorter in a rat compared to humans, an important parameter that needed to be tuned to the data was the time window over which the TICs were compared to each other, starting with the appearance time for every pixel individually [9]. In order to obtain an approximation of the time window, a theoretical calculation of the recirculation time was performed as the time an average red blood cell travels through the circulation of a rat. This recirculation time was estimated to be in the range of 6 to 15 seconds for rats of different kinds and sizes. The spatiotemporal similarity analysis was then performed with time windows of 12, 17, 22, and 27 seconds. A time window of 17 seconds showed to perform best at discriminating malignant tissue from benign. In this paper, only results from this latter analysis are presented.

Before statistical comparison of the correlation coefficient of malignant versus benign tissue, the signal-to-noise ratio (SNR) of the images was assessed: the sum of the signal intensity over time for all pixels was stored as the IDC power, reflecting the overall power of the received signal. Regions with a level of IDC power below a threshold of -22 dBs of the maximum IDC power over all images were excluded from the statistical analysis (shown in black in Fig. 1). This provided a more accurate estimation of the correlation coefficient, limiting the effect of noise. ROIs with comparable signal levels were selected, and the correlation coefficient values were divided into two groups of malignant and benign pixels. Figure 1 shows an example of regions selected for comparison in one of the rats. The image shows a clearly distinguishable tumor, as well as other vascularized regions with a relatively high level of signal.

2) AA: 3D images acquired with AA were used to segment visible vessels, and extract a tortuosity measure. The distance metric (DM), defined as the ratio of the length of the vessel segment to the Euclidian distance between its beginning and end, was evaluated.

D. Statistical analysis

A receiver operating characteristic (ROC) curve was computed for the correlation coefficient to assess its pixel-based classification performance. A higher area under the ROC curve (AUC) corresponds to a better performance of the method. The optimal threshold for separation into two classes (groups) corresponding to either benign or malignant tissue was selected by identifying the minimum Euclidian distance to the upper left corner of the graph.

The correlation coefficient and DM distributions in malignant and benign tissue were compared with the Mann Whitney U test [13] and Kolmogorov-Smirnov test [14]. These tests were chosen because they are nonparametric, making no assumption about the shape of the parameter distribution. This was important because none of the acquired distributions could be approximated with a Gaussian, as derived from the

Kolmogorov-Smirnov test in the one sample case [14], making the common Student t-test inappropriate.

All the image processing and statistical analysis were performed with Matlab software (the MathWorks, Natick, MA).

III. Results

A. Spatiotemporal similarity analysis

The ROC curve generated for the correlation coefficient showed an optimal threshold of 0.17 (illustrated with a black line in Fig. 3) and an AUC equal to 0.98, showing high performance of this method for the current data. Figure 3 shows the distributions for the groups of pixels corresponding to malignant and benign tissue. The distributions show well separated means. Significantly higher ($p<0.01$) mean spatiotemporal similarity was observed for malignant compared to benign pixels according to all statistical tests performed (Table 1). Indeed, the large red area in Fig. 2 belongs to the tumor. Nevertheless, there are a few other areas with correlation coefficient enhancement, as indicated by the numbers in Fig. 2: regions 1, 4, and 5 are present due to the highly reflecting interface of the skin layers. Region 3 has a very low SNR, and indeed is not present among the grey structures in Fig. 1. Vascularized regions with power above the selected threshold in both flanks of the rat exhibit a low correlation coefficient, far from the tumor values.

B. Distance metric

The distributions of the DM are shown in Fig.4. The prevalence of tortuous vessels, indicated by an increased DM, is higher in malignant than in benign tissue. This is also evident from the mean values of the two groups, see Table 1. The Mann-Whitney U test, and the Kolmogorov-Smirnov test showed p-value of 0.004 and 0.002, respectively, rejecting the null hypothesis that the benign and malignant pixels belong to one group.

C. Summary

Table 1 summarizes the results of the statistical analysis. It presents the mean values of the extracted parameters for the malignant and benign regions, as well as the number of samples used and the significance level given by the statistical tests.

Table I: Summary of statistical characteristics of the correlation coefficient and DM distributions.

Parameter	μ_T	μ_C	N_T	N_C	p_1	p_2
DM	1.30	1.22	277	97	0.004	0.002
ρ	0.8	0.3	4460	3883	<0.001	<0.001

μ_T and μ_C refer to the tumor and control groups, stating the mean values of DM and correlation coefficient ρ, respectively. N_T and N_C refer to the number of vessels in tumor and control, in case of DM, and the number of pixels within the selected ROIs, in case of correlation coefficient. p_1 and p_2 represent the significance level of rejection of the null hypothesis for the Mann-Whitney U test and the Kolmogorov-Smirnov test, respectively.

IV. Conclusions and Discussion

Significantly higher mean spatiotemporal similarity and tortuosity was observed for malignant tissue as compared to benign tissue. These results suggest a dependence between dispersion kinetics and vascular tortuosity. The correlation coefficient presents a strong differentiation between benign and malignant tissue: the p-value is low, the distributions for the two groups are centered at different means, and the area under the ROC curve is high (0.98). DM distributions are significantly different according to the non-parametric tests. They have a non-Gaussian shape without a strong separation of means for the two distributions, which may be complex to use alone for cancer prediction, but can complement other features. Indeed, DM is only one of the possible metric reflecting tortuosity. As shown in previous work, the sum of all angles metrics and the volumetric vascular density may provide a stronger differentiation [10]. Therefore, these metrics will be investigated in the future.

Among the shortcomings of our work is the low number of animal models and the fact that selected control regions (benign tissue) chosen from AA and DCE-US data differ. The regions selected for statistical analysis of the correlation coefficient were selected with the condition of a high echo signal. For AA, control regions were selected based on a similar anatomical position as the tumor in the corresponding flank (below the skin, in the center of the image, with an average volume of $4\ \mathrm{cm}^3$). Therefore, direct comparison of DM and correlation coefficient in these regions is not advised.

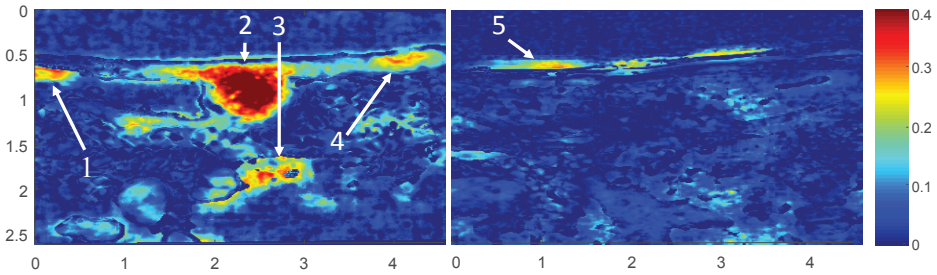

Figure 2: Colormaps of the linear correlation coefficient corresponding to the images in Fig. 1. The tumor is shown as a large red region (arrow number 2). Several regions of enhanced correlation coefficient are indicated by the numbered arrows: regions 1, 4, and 5 are present due to the highly reflecting interface of the skin layers, and were seen in the image before arrival of UCA. Region 3 has a very low signal-to-noise ratio, as can be seen from Fig. 1.

Nevertheless, we were able to observe a trend in agreement with previous observations that malignant tissue has more tortuous vessels as well as a higher correlation coefficient compared to benign [2], [10].

Interestingly, spatiotemporal similarity analysis showed the best results with a time window of 17 seconds. This may indicate that a part of the recirculation curve contains useful information: recirculation may occur earlier in some regions compared to others, and the recirculation shape may be of importance.

Further work will include a longitudinal study of tumor evolution using AA and CUDI. Additional tortuosity measures will also be computed. The heart rate of a rat will be monitored right before the procedure. As a result, a more accurate estimation of the recirculation time for this type of rats will be possible.

ACKNOWLEDGEMENT

This work was supported by the European Research Council Starting Grant (#280209) and the Impulse2 programme within TU/e and Philips. This work was also supported by R01CA170665, R43CA165621, R01CA189479, and T32HL069768 from the National Institutes of Health. P.A.D. declares that he is a co-founder and equity holder of SonoVol, Inc, a company which has licensed intellectual property related to Acoustic Angiography.

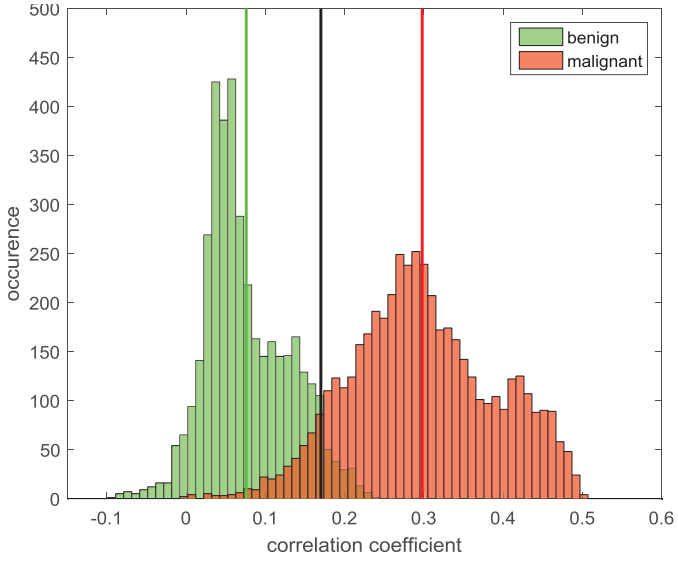

Figure 3: The distributions of the correlation coefficient for malignant and benign tissue with the means of the two distributions indicated with the green and red line, as well as the optimal separation threshold (in black) as identified by the ROC curve.

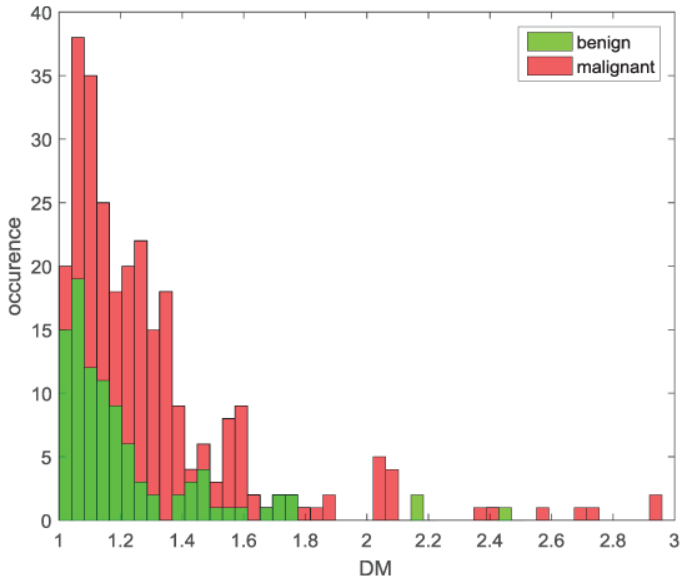

Figure 4: The distributions of the distance metric (DM) for malignant and benign tissue.

REFERENCES

[1] P. Koumoutsakos, I. Pivkin, and F. Milde, "The fluid mechanic of cancer and its therapy," *The Annual Review of Fluid Mechanics*, vol. 45, pp. 325–355, 2013.

[2] M.P.J. Kuenen, T.A. Saidov, H. Wijkstra, and M. Mischi, "Spatiotemporal correlation of ultrasound-contrast-agent dilution curves for angiogenesis localization by dispersion imaging," *IEEE Transactions on Ultrasonic, Ferroelectrics, and Frequency Control*, vol. 60, no. 12, pp. 2665–2669, 2013.

[3] M. P. J. Kuenen, I. H. F. Herold, H. H. M. Korsten, J. J. M. C. H. de la Rosette, and H. Wijkstra, "Maximum-likelihood estimation for indicator dilution analysis," *IEEE Transactions on Biomedical Engineering*, vol. 61, no. 3, pp. 821–831, 2013.

[4] M. Brock, T. Eggert, J. P. Rein, F. Roghmann, K. Braun, L. Bjrn, F. Sommerer, Noldus J., and C. Bodman, "Multiparametric ultrasound of the prostate: Adding contrast enhanced ultrasound to real-time elastography to detect histopathologically confirmed cancer," *The Journal Of Urology*, vol. 189, pp. 93–99, 2013.

[5] E. Quaia, "Assessment of tissue perfusion by conrast-enhanced ultrasound," *European Radiology*, vol. 21, pp. 604–615, 2011.

[6] C. Strouthos, M. Lampaskis, V. Sboros, McNeilly A., and Averkiou M., "Indicator dilution models for the quantification of microvascular blood flow with bolus administration of ultrasound contrast agents," *IEEE Transactions on Ultrasonic, Ferroelectrics, and Frequency Control*, vol. 57, no. 6, pp. 1296–1310, 2010.

[7] M. Mischi, M. P. J. Kuenen, and H. Wijkstra, "Angiogenesis imaging by spatiotemporal analysis of ultrasound-contrast-agent dispersion kinetics," vol. 56, no. 4, pp. 621–629, 2012.

[8] M. P. J. Kuenen, M. Mischi, and H. Wijkstra, "Contrast-ultrasound diffusion imaging for localization of prostate cancer," *IEEE Trans. Med. Imag.*, vol. 30, no. 8, pp. 1493–1502, 2011.

[9] M.P.J. Kuenen, T.A. Saidov, H. Wijkstra, and M. Mischi, "Contrast-ultrasound dispersion imaging for prostate cancer localization by improved spatiotemporal similariy analysis," *Ultrasound in Medicine and Biology*, vol. 39, no. 9, pp. 1631–1641, 2013.

[10] S.E. Shelton, Y. Z. Lee, E. Cherin, F. S. Foster, Aylward S.R., and P.A. Dayton, "Quantification of microvascular tortuosity during tumor evolution using acoustic angiography," *IEEE Signal Processing Magazine*, vol. 25, no. 2, pp. 14–20, 2008.

[11] R.C. Gessner, C.B. Frederick, F.S Foster, and P.A. Dayton, "Acoustic angiography: A new imaging modalityy for asessing microvascular architecture," *International Journal of Biomedical Imaging*, vol. 2013.

[12] RC Gessner, SR Aylward, and Dayton PA, "Mapping microvasculature with acoustic angiography yields quantifiable differences between healthy and tumor-bearing tissue volumes in a rodent model," *Radiology*, vol. 246, no. 3, pp. 733–740, 2012.

[13] H. B. Mann and D. R. Whitney, "On a test of whether one of two random variables is stochastically larger than the other," *The Annals of Mathematical Statistics*, vol. 18, no. 1, pp. 50–60, 1947.

[14] Y. T. Young, "Proof without prejudice:use of the kolmogorov-smirnov test for the analysis of histograms from flow systems and other sources," *The Journal of Histochemistry and Cytochemistry*, vol. 25, pp. 935–941, 1977.